Multi-phase Modeling of the Core Shooting Process

M. Pelzer, A. Ludwig, L. Meiser, P.R. Sahm
Foundry Institute, RWTH Aachen
Intzestr. 5, D-52056 Aachen, Germany

Abstract

The core shooting process is based on the sudden expansion of a limited compressed air volume, which shoots the molding material into the core box with high velocity. Apart from the mould filling the purpose is to release an adequate compression of the molding material. During the entire time it is necessary to draw off the air by means of venting lines, which are situated in the walls of the core box. Thereby, the positioning of the venting lines is of main interest. With the use of a numerical simulation it should be possible to create the core box layouts for every geometry and size without previous time consuming experiments. The simulation presented in this work is based on the iterative solution of a two phase flow, in which the fluid phase is air and the solid phase is granular. The Eulerian formulation serves as a basis of design, which treats both phases as a continuum. The coupled differential equations to be resolved are, for one the continuity conservation equations (mass balances) and, secondly the momentum conservation equations for both phases. Fundamental knowledge about the flow behavior in the core box is necessary to carry out this simulation. The volume fraction of the sand and the entry velocity into the core box of both phases must be determined experimentally. With these boundary conditions first two dimensional simulation results are available for different geometries.

Modeling of Casting, Welding and Advanced Solidification Processes IX
Edited by Peter R. Sahm, Preben N. Hansen and James G. Conley

1. Introduction

The core shooting process is based on the sudden expansion of compressed air with which a granular molding material, usually sand coated with an organic binder, is then shot into the core box at an high velocity. Apart from sufficient filling of the box, compression of the molding material must also be adequate. During the entire shooting process it is necessary to draw off the air from the core box. This is achieved by the use of venting lines situated at adequate positions in the walls of the box. Naturally, the location and the size of the venting lines are essential for a proper process. Thus, numerical modeling of the core shooting process is a great help in planning optimal process realization without performing time consuming experimental investigations.

The numerical simulations presented in this paper are performed with the commercial CFD-software Fluent (V. 4.5.1). It is based on the iterative solution of a two-phase flow formulation in which the first phase, denoted as "fluid", is assumed to be the air and the second phase, denoted as "granular", the molding material sand. As both phases are treated as a continuum the Eulerian formulation of the conservation equations for momentum and mass is used. In contrast to the common Eulerian two-phase approaches special emphasis must be placed (i) on an additional pressure term for the granular phase, namely the "solid pressure", (ii) on the viscosity formulation for the granular phase taking into account the complex interaction of the sand, (iii) on the formulation for the momentum exchange between air and sand, and (iv) on adequate wall boundary conditions for the granular phase. Details of these items are given below.

In order to obtain information on the boundary conditions for the numerical simulations the volume fraction and the velocity of the sand at the entrance of the core box had to be determined experimentally. As a first step we considered a simple cylindrical core box for the experimental work and the numerical simulations and proceeded then to more complex geometries.

2. Experimental Work

The cylindrical core box had a diameter of 140 mm and a height of 260 mm. Seven venting lines were placed at the bottom. One on the axis and the others at a distance of 50 mm from the axis symmetrically arranged. They had a diameter of 16 mm and formed an array with 7 parallel lamellae. The sand cylinder had a volume of 4 liter. The selected diameter of the round opening between the sand cylinder and the core box (shooting heat) was 16 mm. The molding material was sand coated with a cold box binding system. The sand had an average grain size of 240 μm. A pressure of 3 bar was applied for shooting the sand into the core box.

In order to determine the velocity of the sand, a box with an acrylic glass window was placed under the shooting head. The sand cylinder was filled with several layers of colored sand. The shooting process was filmed with a video recorder. From optical observation of the movement of colored segments the velocity of the sand was measured to be about 17.6 m/s. For the simulation it is assumed that the air and the sand entered the core box with the same velocity.

The volume fraction of the sand was determined by measuring the time taken to fill a core box made of glass with a video camera (Fig.1). It was assumed a constant mass flux at the entrance throughout the process. The sand fraction of the entering jet was 65.73 %.

To visualize the filling process, differently colored sand was arranged in layers within the sand cylinder and then shot into a cylindrical core box. Afterwards the core was hardened and sawn along the cylindrical axis. The resulting colored sand pattern showed that the filling revealed some turbulence at the walls, but for most of the process the flow was not turbulent leading to the regular convex sand layering (see Fig.2).

3. Model Description

A two-phase flow can be modeled by considering the two phases as a continuum and applying the conservation of mass and momentum for each of them. The corresponding equations are:

$$\frac{\partial}{\partial t}(\alpha_q \rho_q) + \nabla(\alpha_q \rho_q \vec{u}_q) = 0 \tag{1}$$

$$\frac{\partial}{\partial t}(\alpha_q \rho_q \vec{u}_q) + \nabla \cdot (\alpha_q \rho_q \vec{u}_q \otimes \vec{u}_q) = -\alpha_q \nabla p + \nabla \cdot \bar{\bar{\tau}}_q + \alpha_q \rho_q \vec{g} + K_{pq}(\vec{u}_p - \vec{u}_q) + \vec{F}_q \tag{2}$$

where α_q is the fraction, ρ_q the density, $\vec{u}_q$ the velocity, $\vec{F}_q$ an additional body force and τ_q the strain tensor of phase *q*. $\vec{g}$ is the gravitational acceleration and *p* the pressure. For the core shooting process air is considered to be the first phase (named "fluid" (f)) and sand the second phase (named "granular" (g)).

To account for the special nature of the sand-air mixture it is necessary to model the dynamic of sand motion. For this an analogy between the random particle motion arising from particle-particle collisions and the thermal motion of molecules in a gas is drawn. As regards gases, the intensity of the particle velocity fluctuations determines the stresses, the viscosity, and the pressure of the granular phase. It is assumed that after fluidization the sand particles reveal a Maxwellian velocity distribution. The characterizing "pseudo-temperature" is called granular temperature θ_g. It is proportional to the mean square of random motion of particles and associated with the kinetic energy of the sand.

3.1. Momentum Exchange Term

Momentum exchange between the air and the sand is considered by adding the term $K_{gf}(\vec{u}_g - \vec{u}_f)$ to the momentum conservation equations (Eq.(2)). For the momentum exchange coefficient K_{gf} we used a form derived by Syamlal and O'Brien [1, 2]:

$$K_{gf} = \frac{3\alpha_g \alpha_f \rho_f}{4 v_{rg}^3 d_g} C_D \mathrm{Re}_g \left| \vec{u}_g - \vec{u}_f \right| \tag{3}$$

Here Re_g is the relative Reynolds number [3], C_D the drag coefficient proposed by Dalla Valle [4], d_g the particle diameter of the solid phase (assumed to be 240 µm) and v_{rg} the terminal velocity correlation of the solid phase [5]. The approach of Syamlal and O'Brien is based on measurements of the terminal velocity correlation of particles in fluidized or settlings beds.

3.2 Solid Pressure

For granular flows in the compressible regime a solid pressure p_g is calculated (independently from the pressure of the air) and used as an additional body force in form of a pressure gradient term in the granular phase momentum equation. As it is assumed that the motion of sand follows the granular kinetic theory with collision, p_g is composed of a kinetic term and a term due to particle collisions as:

$$p_g = \alpha_g \rho_g \theta_g + 2\rho_g (1 + e_{gg}) \alpha_g^2 g_{0gg} \theta_g \tag{4}$$

where e_{gg} is the coefficient of restitution for the particle collisions (sand specific) and g_{0ss} is the radial distribution function. The latter is a correction factor that modifies the probability of collisions between sand particles when the granular phase becomes dense. For e_{gg} we used 0.8 and for g_{0gg} the semi-empirical expression derived in [6]:

$$g_{0gg} = 3/5 \cdot \left[1 - \left(\alpha_g / \alpha_{g,\max}\right)^{0.33}\right]^{-1} \tag{5}$$

It is obvious that Eq. (5) describes the transition from "compressible" conditions with $\alpha < \alpha_{g,max}$, where the spacing between the sand particles can continue to decrease, to the "incompressible" condition with $\alpha = \alpha_{g,max}$, where no further decrease in the spacing can occur. $\alpha_{g,max} = 0.6$ was used in the present work.

3.3 Shear Stresses for the Granular Phase

The stress tensor for the granular phase contains shear and bulk viscosities arising from particle momentum exchange due to translation and collision. The shear viscosity μ_g is assumed to consist of a collisional and kinetic part. The collisional part is based on a formulation derived in [3, 7], and the kinetic part is based on a formulation derived in [7].

$$\mu_{g,col} = \frac{4}{5}\alpha_g \rho_g d_g g_{0gg}(1+e_{gg})\left(\frac{\theta_g}{\pi}\right)^{0.5} \tag{6}$$

$$\mu_{g,kin} = \frac{10\rho_g d_g \sqrt{\theta_g \pi}}{96\alpha_g (1+e_{gg}) g_{0gg}}\left(1+\frac{4}{5}g_{0gg}\alpha_g(1+e_{gg})\right)^2 \tag{7}$$

For the granular bulk viscosity a formulation is used which is based on the same concept as for $\mu_{g,col}$:

$$\lambda_g = \frac{4}{3}\alpha_g \rho_g d_g g_{0gg}(1+e_{gg})\left(\frac{\theta_g}{\pi}\right)^{0.5} = \frac{5}{3}\mu_{g,col} \tag{8}$$

This approach accounts for the resistance of the particles against the compression and expansion used. In dense flow at low shear, where the volume fraction for the granular phase approaches the packing limit, the generation of stress is mainly due to friction between the particles. The granular shear viscosity computed from kinetic theory does not, by default, account for the friction between particles. To include the frictional particle-particle effects in very dense flows, a frictional viscosity is introduced into the stress-strain tensor. Thus, the effective viscosity is composed of the viscous part, μ_s, from granular kinetic theory, and the frictional part, $\mu_{s,fric}$, based on the Coulomb yield criterion (described in any soil mechanics handbook). We chose with [8] the following approach:

$$\mu_{g,eff} = \begin{cases} \max(\mu_g, \mu_{g,fric}) & \alpha_g \geq 0.98 \cdot \alpha_{g,\max} \\ \mu_g & \alpha_g < 0.98 \cdot \alpha_{g,\max} \end{cases} \tag{9}$$

3.5 User Defined Subroutines

Due to comparison of the simulation results and real experimental findings (Fig.2) a discrepancy between reality and simulation became obvious. The friction viscosity, which becomes active in (Eq. (9)) at 98 % of the maximal packing limit the calculation of the viscosity of the granular phase, is limited within the program to 5000 Pas. Generally, this delimitation is necessary, since for very small velocity gradients the friction viscosity term would diverge. Within Fluent it is possible to intervene by user-defined subroutines directly. In order to increase the delimitation for the friction viscosity implemented in the program, the viscosity of the second phase had to be programmed completely new. That includes both, the viscosity for weakly loaded granular flows as well as the viscosity for strongly loaded ones. The viscosity is limited within our user-defined subroutines to 30000 Pas.

3.4 Wall Boundary Conditions

In the Jackson-Johnson condition [9], the velocity of the granular phase at a wall is formed by setting the lateral momentum flux transmitted to the boundary by particle collisions equal to the tangential stress exerted by particle adjacent to the wall. The tangential stress exerted on the boundary by the granular phase is thus the product of the change of momentum per particle collision, the collision frequency, and the number of particles per unit area adjacent to the wall. For the granular temperature the flux of granular temperature to the wall is balanced by the energy dissipation at the wall due to inelastic particle-wall collisions [10]. The Jackson-Johnson wall boundary condition [10] was used as velocity boundary condition for the granular phase and for the granular temperature.

4. Results and Discussion

Assuming rotation symmetry, two- dimensional simulations of the core shooting process for the simple cylindrical configuration described in section 2 are performed (Fig.3). The initial conditions as well as the boundary conditions at the inlet are taken from experimental facts. The experimental investigations showed that the core shooting process proceeds as follows. A convergent jet consisting of about 65.73% sand enters the core box. Its diameter corresponds to the diameter of the opening in the shooting heat. This finding is reproduced by the simulation (see Fig. 1 and Fig. 3). Due to air resistance the jet reveals a mushroom-like tip. This phenomenon is hardly reproduced by the simulation. The reason for this may be on an insufficient description of the momentum transfer for the interaction between the free jet and the air. After the jet has hit the bottom of the core box the sideward spread is accomplished by the same turbulent vortices. Here the assumption of lamellar flow in the model is incorrect. However, the turbulent filling is restricted only to the very beginning of the process. The major volume fraction of the cavity is filled with lamellar flow of sand (Fig.2). During this stage of the process regular concave sand layers are formed. The simulation reproduces the concave shape of the interface air/sand quite well. While the core box becomes more and more filled with sand, the air flows through sand towards the venting lines (Fig.4). After the successful simulation of the cylindrical geometry, a more complex core with a turn- around ("horseshoe" –shaped core) has been produced. Directly behind the turn around a defect was found (Fig.5a)). The corresponding simulation showed that in this area the compression was poor (Fig. 5b)). This result encourages us to believe that the used approach is reasonable and that further efforts are worth to be carried out.

5. Conclusions

The main conclusions of this work are:

- Although core shooting is a highly complex industrial process, it can be modeled with an adequate two-phase formulation in which the fluid phase air and the granular phase sand both can be treated as a continuum.

- However special emphasis must be placed on the formulations for (i) the viscosity of the granular phase, (ii) the momentum exchange between the air and the sand, (iii) the additional pressure on the sand arising from the interaction between the sand particle, and (iv) the boundary conditions for the granular phase.
- For simple cylindrical geometry the numerical results are in sufficient agreement with experimental observations.
- Applying the simulation to a more complex geometry results in reasonable predictions of defects

Acknowledgement

This work was supported by the "Deutsche Bundesstiftung Umwelt", "Röperwerk-Gießereimaschinen GmbH", "Ashland-Südchemie-Kernfest GmbH" which the authors gratefully acknowledge.

References

[1] Syamlal M., O'Brien T.J.: in "A Generalized Drag Correlation for Multiparticle Systems", Unpublished report (1986)
[2] Syamlal M., Rogers W., O'Brien T.J.: in "MFIX Documentation: Volume 1, Theory Guide", DOE/METC-9411004, NTIS/DE9400087, National Technical Information Service, Springfield, VA, (1993)
[3] Richardson J.R., Zaki W.N., Trans. Inst. Chem. Eng. 32 (1954) pp. 35-53
[4] Dalla Valle J.M.: in "Micromeritics", Pitman, London (1948)
[5] Garside J., Al-Dibouni M.R., I & EC Process Des. Dev. 16 (1977) pp. 206-214
[6] Ding, J. and Gidaspow, D., "A Bubbling Fluidization Model Using Kinetic Theory of Granular Flow," AIChE J. 36(4) (1990) pp. 523-538
[7] Gidaspow D., Bezburuah R., Ding J., Proceedings of the 7th Engineering Foundation Conference on Fluidization (1992) pp. 75-82
[8] Schaeffer D.G., J. Diff. Eq. 66 (1987) pp. 19-50
[9] Sinclair J.L., Jackson R., AIChE J. 35(9) (1989) pp. 1473-1486,
[10] Johnson P.C., Jackson R., J. Fluid Mech. 176 (1987) pp. 67-93

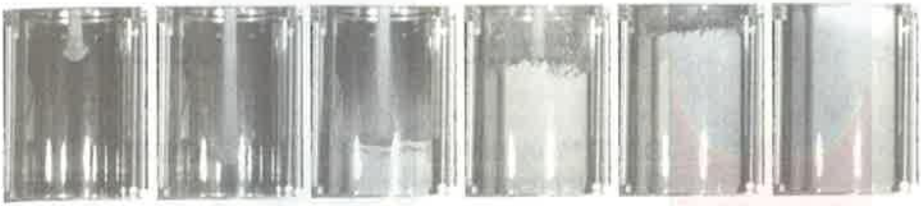

Figure 1: Visualization of the core shooting process with the aid of a video equipment. The time interval between the pictures is not constant. Geometrical dimensions and applied process conditions are specified in section 2.

Figure 2: Differently colored sand was arranged in layers within the sand cylinder and then shot into a cylindrical core box. The initial color sequence was brown (black), yellow (light gray), green (dark gray), orange (medium gray), white and then again brown, yellow, green, orange.

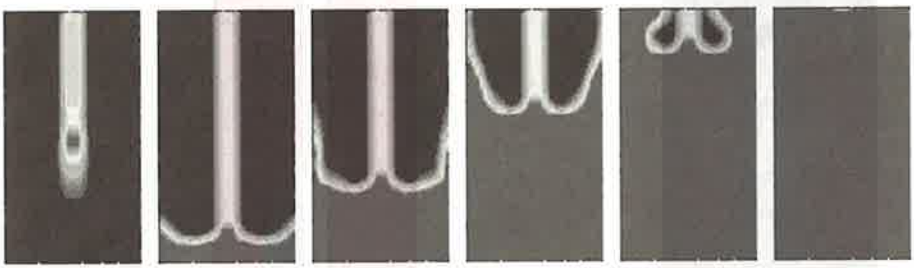

Figure 3: Simulated filling sequence for the core shooting process shown in Fig.2. Red (dark gray) represents the packing limit of sand and blue (black) regions without sand. Orange (light gray) represents a sand volume fraction of 65.73 %.

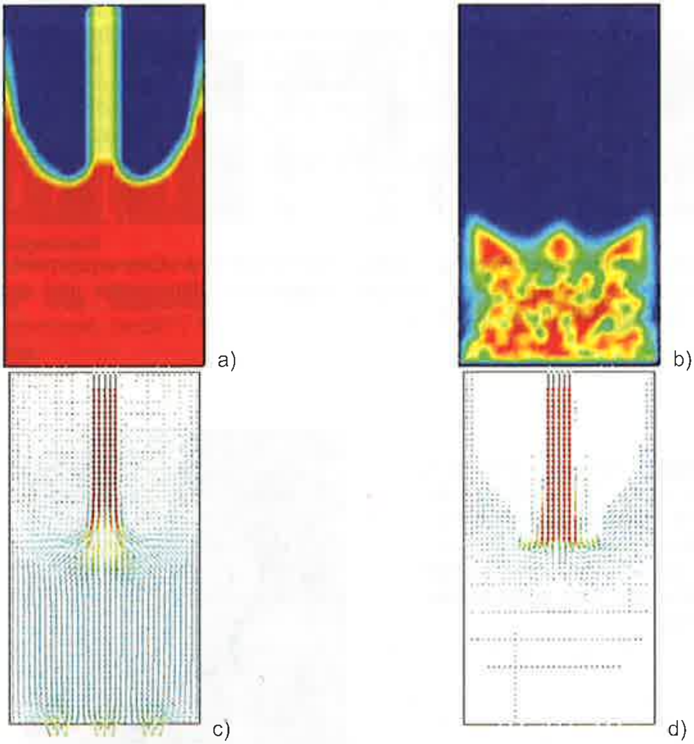

Figure 4: Comparison of the filling (a), the viscosity distribution of the granular phase (b), the velocity of air (c) and the velocity of the sand (d) at a filling level of about 70 %. Note that the air leaves the core box by flowing through the compressed sand layer towards the venting lines. In the compressed sand layer the granular viscosity reveals high values of about 30000 Pas.

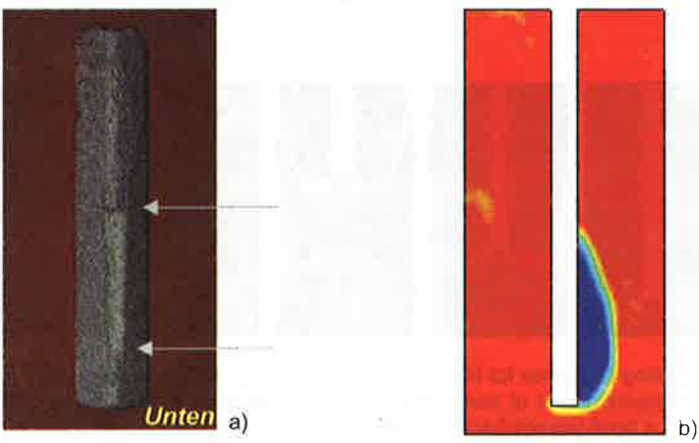

Figure 5: Comparison between a "horseshoe" shaped core (a) and the simulation of the corresponding area (b). The simulation predicts an insufficient sand compression at the position where the real core reveals the defect.